Research article

Crystallization behavior and ionic conductivity of NASICON type glass-ceramics containing different amounts of B_2O_3

Banafsheh Zarabian [a], Bijan Eftekhari Yekta [a], Sara Banijamali [b,*]

[a] *School of Metallurgy & Materials Engineering, Iran University of Science and Technology, Tehran, Iran*
[b] *Ceramic Department, Materials and Energy Research Center (MERC), Alborz, Iran*

A B S T R A C T

In this research, glass-ceramics belonging to the system of Li_2O-TiO_2-P_2O_5 were prepared by the addition of different amounts of B_2O_3. The glass formation ability of the starting glass materials along with the crystallization trend as well as ionic conductivity of the corresponding glass-ceramics were also examined. Starting glasses were obtained through the melt quenching technique and glass-ceramics specimens were prepared through one-step heat treatment. The glass-ceramic samples were then examined through X-ray diffractometry, differential thermal analysis, electrochemical impedance spectroscopy, and scanning electron microscopy. According to the obtained results, the addition of a 2.5 mol% of B_2O_3 to the glass composition led to a sharp increase in ionic conductivity at room temperature. So that the bulk conductivity of the specimen heat treated at 950 °C for 2 h was measured to be 1.17×10^{-3} Scm^{-1}, which was 10 times bigger than that of the base glass-ceramic with no additive. It also decreased the crystallization temperature and viscosity of the parent glass, resulting in increased crystallinity while further addition of B_2O_3 drained the conductivity and crystallinity of glass-ceramics.

1. Introduction

Lithium ion conducting batteries have drawn great attention owing to their high energy density, low thermal expansion difference between electrodes and electrolytes, low weight and high ionic conductivity [1–3]. NASICON type ceramics are of great potential to be used as electrolytes in the new generation of lithium ion conducting batteries. Among them, glass-ceramics have been introduced since they do not have grain boundaries and hence will not drain conductivity [4–10]. NASICON glass-ceramics belonging to the system of Li_2O-Ti_2O-P_2O_5 have shown superior ionic conductivity. The main phase in this system is lithium titanium phosphate ($LiTi_2(PO_4)_3$) with the NASICON structure. This structure is like $N[A_2B_3O_{12}]$, where N is a cation such as Li and Na, A is a cation such as Ge, Ti, Sn, Hf, and Zr, and B is a cation such as P and Nb. The structure of NASICON material is made of two AO_6 hexagonal and three BO_4 octahedral, which make some paths for Li ions to move easily and create ionic conductivity [7, 11, 12].

However, glass formation besides suitable crystallization behavior using the stoichiometric composition of $LiTi_2(PO_4)_3$ has always been challenging. A solution to obtain adequate glass forming ability besides keeping enough crystallization of the NASICON phase is an accurate modification of initial glass compositions. If this modification could improve the simultaneous glass forming ability and the final glass-ceramic materials' ionic conductivity that can be a big discovery [13, 14]. It has been reported that the addition of 5 mol% of B_2O_3 to the glasses with the stoichiometric composition of $Li_{1.5}Al_{0.5}Ge_{1.5}(PO_4)_3$ not only leads to an increase in the relative glass and glass-ceramic conductivity but also improves glass-formation [14, 15].
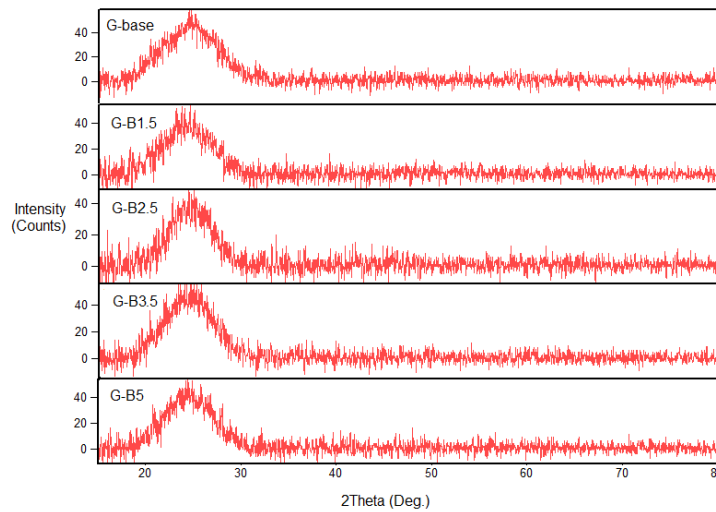
Fig. 1. Annealed starting glasses' XRD patterns.

Therefore, the main idea of the current research aims to study the influence of B_2O_3 addition on the ionic conductivity and crystallization behavior of NASICON type glass-ceramics containing different amounts of B_2O_3.

2. Experiments

The melt-quenching technique was employed to fabricate the starting glasses. The base glass chemical composition was chosen on the basis of the stoichiometric composition of $LiTi_2(PO_4)_3$ containing 12.5 Li_2O, 50 TiO_2, and 37.5 P_2O_5 (in mol%). To obtain B_2O_3 containing glasses, 1.5, 2.5, 3, and 5 mol% of B_2O_3 were added to the composition of the base glass. The obtained glass specimens were respectively named G-base, G-B1.5, G-B2.5, G-B3.5, and G-B5.

The starting Precursor materials contained Li_2CO_3 (Merck 808); TiO_2 (Merck 5671); $NH_4H_2PO_4$ (Merck 101126); H_3BO_3 (Merck 100165); and high purity SiO_2. The homogeneously mixed batches were transferred to the electric furnace (Azar 1720) and meted in the fused silica crucibles. The furnace temperature was increased to 1500 °C and maintained for 20 minutes at the maximum temperature to obtain homogeneous melts. Then, the molten glasses were poured onto a cold plate made of stainless steel and immediately pressed by another plate. All fabricated glasses were annealed for 2 h at 500 °C to release stress and then cooled down to ambient temperature.

Differential thermal analysis (Polymer Laboratories) was carried out to monitor the role of the B_2O_3 additive on the crystallization behavior of studied glasses at the heating rate of 10 °C/min in air. X-ray diffraction (XRD) patterns of all glass and glass-ceramic specimens were obtained using the Siemens D500 diffractometer in the 2θ range of 2 ° to 80 °. Crystalline phases were identified by means of X'Pert HighScore Plus 2.1 software. Scanning electron microscopy (SEM, Vega TESCAN) was used for microstructural observations. Prior to SEM analysis, all glass-ceramic specimens were etched chemically through immersion in the HF dilute solution for a few seconds and were afterward coated by a gold thin layer.

The AC impedance of all glass-ceramics was measured in the 100-mV voltage amplitude and frequency range of 1 Hz to 1 MHz. The samples' opposite faces were coated with gold to have proper electrical contact. Subsequently, the samples were assembled into a cell employing blocking electrodes made of stainless steel resulting in the impedance spectrometer. The glass-ceramics ionic conductivity was obtained from the AC impedance spectrum at room temperature with respect to their cross-sectional area and thickness.

3. Results and discussion

The starting glasses' XRD patterns are shown in Fig. 1 after annealing. It can be seen that all glasses are completely amorphous as far as the
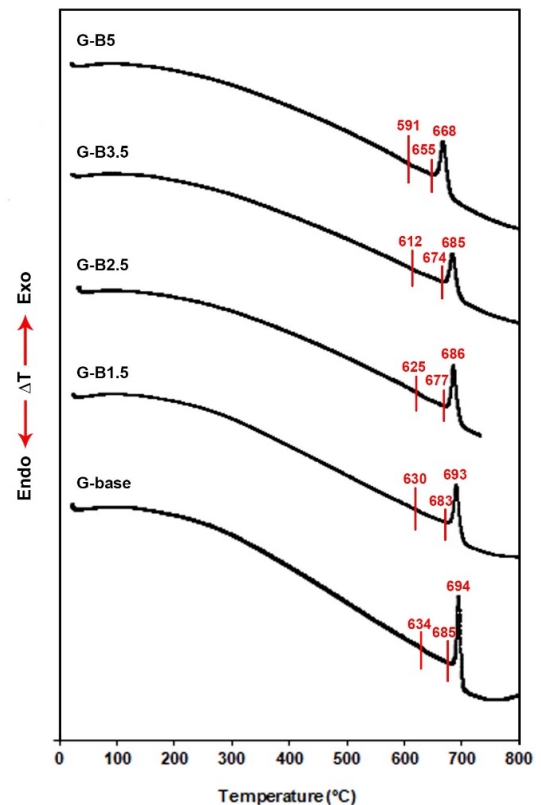

Fig. 2. Annealed starting glasses' DTA results at the 10 °C/min heating rate.
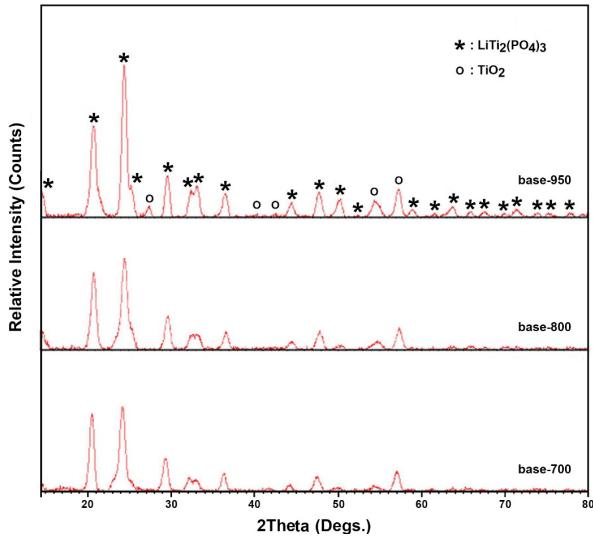
Fig. 3. XRD spectra of the G-Base glass-ceramics after 2 h one-step heat treating at 700, 800, and 950 °C and the 10 °C/min heating rate.

Table 1. Measurements of glass formation ability based on the Dietzel and Paulin methods (The temperatures are in °C).

Glasses	T_g	T_x	T_c	$T_c - T_x$	$T_x - T_g$	S	ΔT
G-Base	634	685	694	9	51	0.72	60
G-B1.5	630	683	693	10	53	0.84	63
G-B2.5	625	677	686	9	52	0.74	61
G-B3.5	612	674	685	11	62	1.14	73
G-B5	591	655	668	13	64	1.41	77

main glass and its further increase, both crystallization temperature (T_c) and glass transition temperature (T_g) are shifted to the lower temperatures.

Based on the DTA analysis, the glass formation ability of the studied glass compositions was accordingly determined based on the Dietzel and Paulin methods [16, 17] as the following equations:

$$\Delta T = (T_c - T_g) \tag{1}$$

$$S = (T_x - T_g)(T_c - T_x)/T_g \tag{2}$$

where ΔT and S are both showing the glass-formation ability of melt in quenching, that is the crystallization resistance of the glass in heating. The higher the amount of these two factors, the greater the glass-formation ability of the melt. In these equations, T_g, T_x, and T_c are respectively referred to as the glass transition, onset of crystallization peak, and crystallization peak temperatures. The relevant
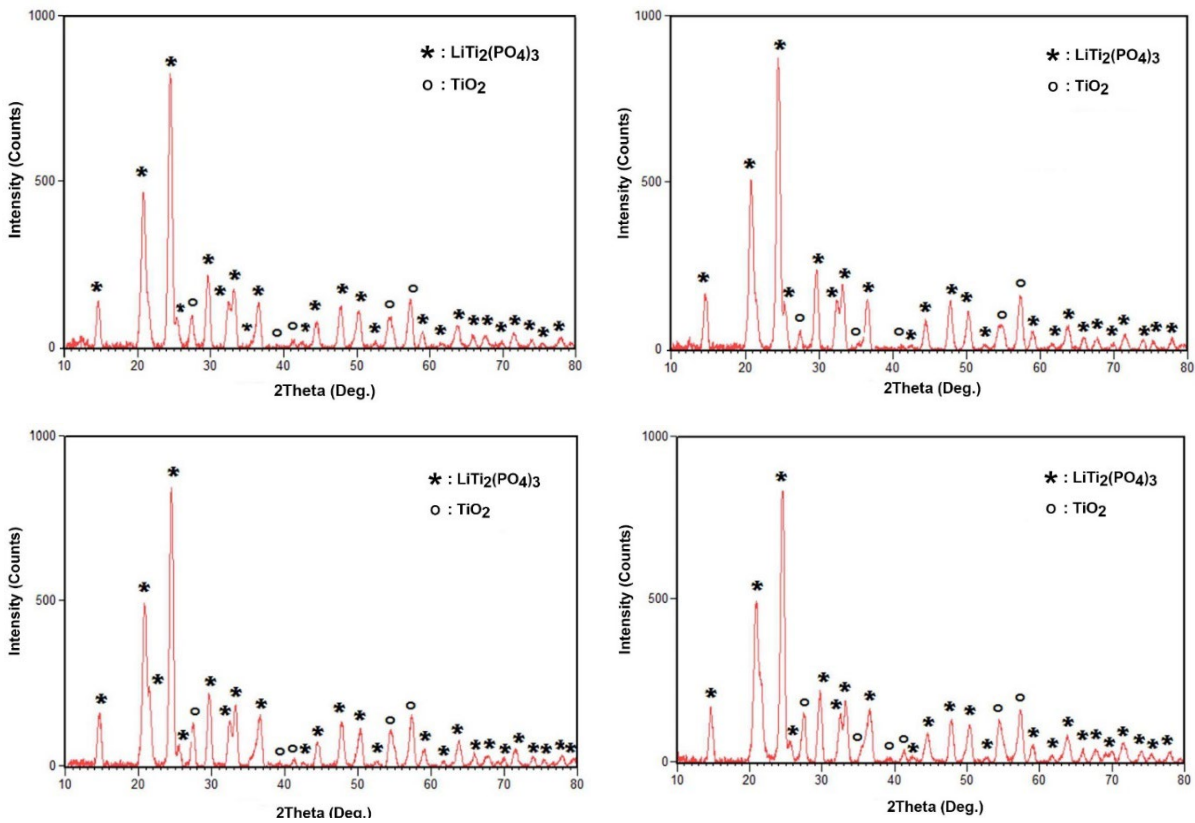
device can tell. The obtained glasses were transparent and violet, due to the Ti^{3+} ions present in the glass.

Fig. 2 shows the starting glasses' DTA thermographs at the 10 °C/min heating rate. It can be deduced from Fig. 2 that by B_2O_3 addition to the

Fig. 4. XRD spectra of B_2O_3 containing glass-ceramic materials heat processed at 950 °C for 2 h with the 10 °C/min heating rate: a) G-B1.5, b) G-B2.5, c) G-B3.5, and d) G-B5.
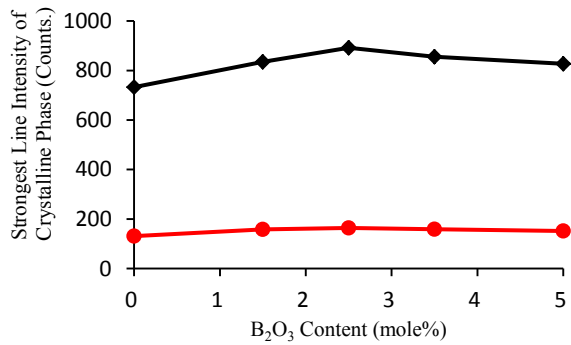
Fig. 5. Changes in the strongest line intensity of each crystalline phase (taken from XRD patterns) of B_2O_3 containing glass-ceramics versus B_2O_3 content ($\blacklozenge$: $LiTi_2(PO_4)_3$, $\bullet$: TiO_2).

measurements have been summarized in Table 1. According to the Paulin and Dietzel measurements, two glasses of G-B3.5 and G-B5 have the greatest amount of ΔT and S, meaning the best glass formation ability. They are expected to be the most resistive against crystallization in the subsequent heat treatment.

Fig. 3 shows the XRD patterns of the G-Base glass-ceramics after one-step of heat treatment at 700 (near crystallization peak temperature), 800, and 950 °C for 1 h at the 10 °C/min heating rate. As can be seen, TiO_2 and $LiTi_2(PO_4)_3$ are present as the minor and major crystalline phases. The increase in processing temperature from 700 °C to 950 °C has enhanced the peak intensity of crystallized phases, which could be related to the increased crystallinity of glass-ceramic specimens or the growth of crystallographic planes. Both statuses can provide better mobility for Li^+ ions to pass through the channels in the NASICON structure and increase ionic conductivity [18]. Therefore, the highest temperature of heat treatment (950 °C) was considered for further heat treatments.

Fig. 4 represents the XRD patterns of B_2O_3 containing specimens after one-step heat treatment at 950 °C and the 10 °C/min heating rate for 2 h. It is obvious from this figure that the addition of B_2O_3 does not have a strong influence on the crystallization behavior of these glass-ceramics and all of them follow the same crystallization trend having slight differences in the intensity of crystalline phases. The main crystalline phases in all specimens were identified as $LiTi_2(PO_4)_3$ and TiO_2. Interestingly, B_2O_3 totally remains in the residual glass matrix of all heat treated specimens and does not contribute to the structure of crystalline phases.

The changes in the intensity of the strongest peak lines of both crystallized phases in the glass-ceramics containing various amounts of

Table 2. Measurements of resistance and ionic conductivity of fabricated glass-ceramics at 298 K.

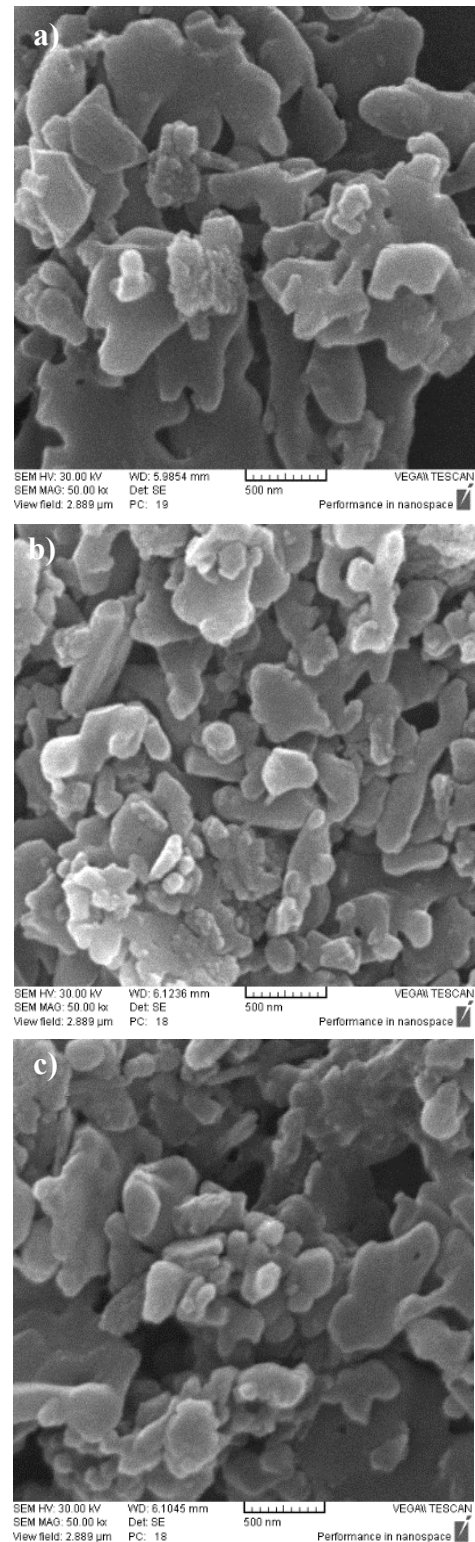| Glass-ceramic	R_t (ohm)	R_b (ohm)	σ_t (Scm^{-1})	σ_b (Scm^{-1})
G-Base	2.92×10^4	1.83×10^3	6.83×10^{-6}	1.09×10^{-4}
G-B1.5	1.62×10^3	7.76×10^2	2.04×10^{-4}	4.25×10^{-4}
G-B2.5	4.07×10^3	14.34×10^2	4.12×10^{-4}	1.17×10^{-3}
G-B3.5	1.67×10^3	5.53×10^2	1.19×10^{-4}	3.61×10^{-4}
G-B5	1.55×10^3	6.04×10^2	8.99×10^{-5}	2.30×10^{-4}

Fig. 6. SEM images of the a) G-Base, b) G-B2.5, and c) G-B5 glass-ceramic materials heat-processed for 2 h at 950 °C.

B_2O_3 have been shown in Fig. 5. As can be observed, the addition of B_2O_3 up to 2.5 mol% could increase the crystallization of the NASICON phase, while the crystallization of the second phase hasn't changed, considerably. Further addition of B_2O_3 decreased the
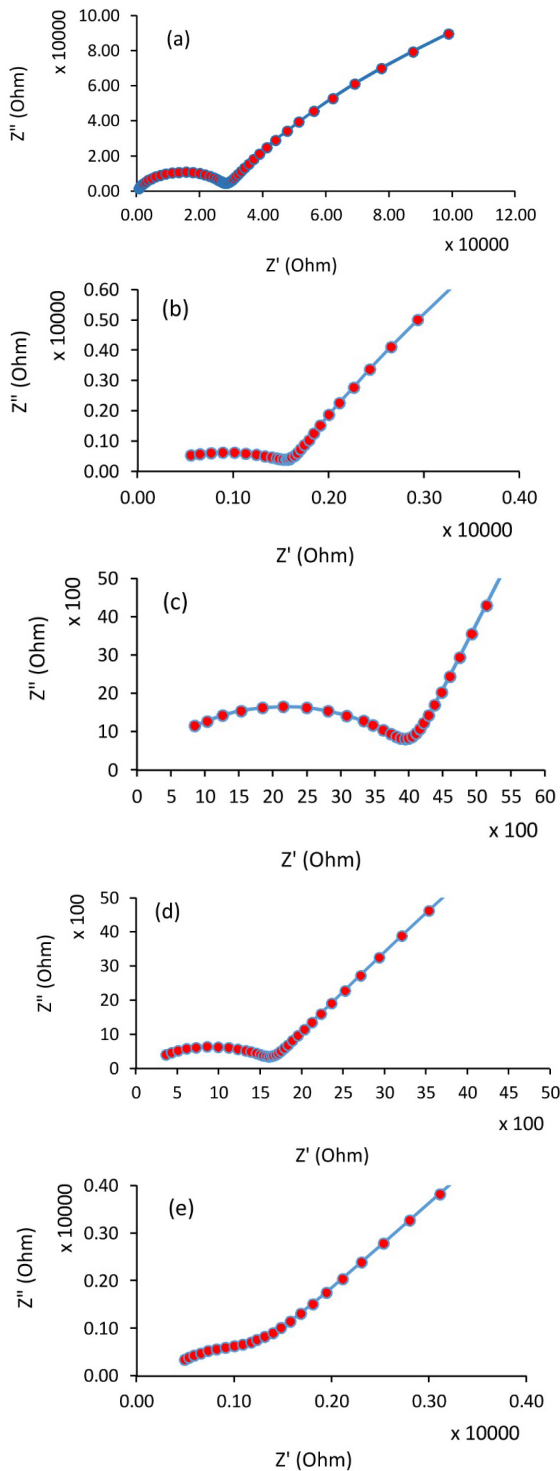
Fig. 7. Impedance spectra taken at 298 K from glass-ceramic materials heat treated for 2 h at 950 °C: a) G-Base, b) G-B1.5, c) G-B2.5, d) G-B3.5, and e) G-B5.
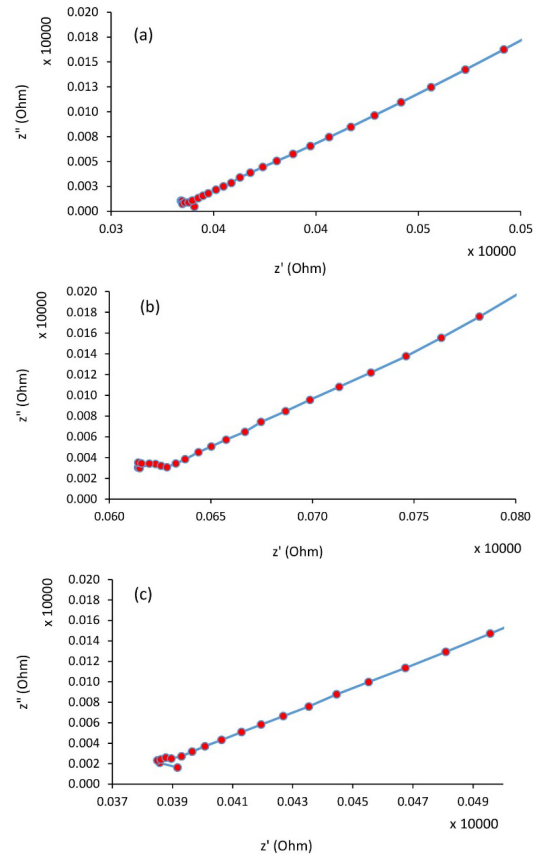

Fig. 8. Impedance spectra taken at 298K from starting glasses: a) G-Base, b) G-B1.5, and c) G-B3.5.

In Fig. 6, SEM micrographs of G-Base, G-B2.5, and G-B5 glass-ceramics heat treated for 2 h at 950 °C are shown. It could be seen that the crystalline phases have semi-spherical morphology. Furthermore, it seems that crystallinity has been enhanced in the microstructure of G-B2.5 glass-ceramic.

The impedance spectra taken at 298 K for all glass-ceramic samples processed at 950 °C for 2 h are presented in Fig. 7. The presence of one semi-circle indicates there is just one conducting phase in these glass-ceramic. In each spectra, total (R_t) and bulk resistance (R_b) were accordingly obtained from the interception points of the relevant plot with the horizontal axis in low (right part of the semi-circle) and high (left part of the semi-circle) frequencies. Afterward, the ionic total (σ_t) and bulk (σ_b) conductivities were calculated using the Eq. 3:

$$\sigma = t/AR \qquad (3)$$

in which A, t, and R are the area, thickness, and resistance of the sample, respectively [19]. These measurements have been summarized in Table 2.

It could be seen that the addition of B_2O_3 up to 2.5 mole fraction has increased the bulk conductivity of glass-ceramic G-B2.5 (1.17×10^{-3} Scm^{-1}), considerably that is believed to be due to the higher crystallinity of this specimen. Since the activation energy for lithium ion conduction in the NASICON structures is lower than that of the corresponding glasses [11], the more the crystallized NASICON phase the higher the conductivity.

crystallinity of the NASICON phase which is believed to be related to their higher glass-forming ability. However, all glass-ceramics containing B_2O_3 show greater crystallinity which is related to the lower viscosity of melts containing B_2O_3 content.

The impedance spectra taken at 298 K for three starting glasses are shown in Fig. 8. The absence of semi-circles in these spectra confirms that the glassy phase does not contribute to the ionic conductivity and the presence of NASICON crystalline phase is responsible for ionic conductivity of glass-ceramics specimens, as discussed earlier.

4. Conclusions

- The base and B_2O_3 including glass-ceramic materials were successfully manufactured via one-step heat treating process. All glass-ceramics contained lithium titanium phosphate (with the NASICON structure) as the major crystalline phase.
- Addition of 1.5 to 5 mol% of B_2O_3 decreased the crystallization temperature about 30 °C.
- Addition of more than 2.5 mol% of B_2O_3 improved glass forming ability and declined crystallinity of the relevant glass-ceramics.
- The highest conductivity of 1.17×10^{-3} Scm^{-1} was achieved at 300 K for the G-B2.5 specimen crystallized at 950 °C for 2 h.

CRediT authorship contribution statement

Banafsheh Zarabian: Investigation, Formal Analysis, Methodology, Writing – original draft.

Bijan Eftekhari Yekta: Supervision, Funding acquisition, Project administration, Resources.

Sara Banijamali: Supervision, Writing – review & editing, Project administration, Software.

Data availability

The data underlying this article will be shared on reasonable request to the corresponding author.

Declaration of competing interest

The authors declare no competing interests.

Funding and acknowledgment

References

[1] B. Scrosati, J. Garche, Lithium batteries: Status, prospects and future, J. Power Sources. 195 (2010) 2419–2430. https://doi.org/10.1016/j.jpowsour.2009.11.048.

[2] F. Maisel, C. Neef, F. Marscheider-Weidemann, N.F. Nissen, A forecast on future raw material demand and recycling potential of lithium-ion batteries in electric vehicles, Resour. Conserv. Recycl. 192 (2023) 106920. https://doi.org/10.1016/j.resconrec.2023.106920.

[3] S.V. Gaslov, M.S. Rublev, A.E. Biryukov, S.O. Kopytov, Virtual simulation of the operation of a lithium-ion battery as a part of a vehicle using ID complex model, Transport. Res. Procedia 68 (2023) 906–916. https://doi.org/10.1016/j.trpro.2023.02.127.

[4] I. Abrahams, E. Hadzifiejzovic, Lithium ion conductivity and thermal behaviour of glasses and crystallised glasses in the system Li2O-Al2O3-TiO2-P2O5, Solid State Ion. 134 (2000) 249–257. https://doi.org/10.1016/S0167-2738(00)00768-2.

[5] T. Minami, Fast ion conducting glasses, J. Non-Cryst. Solids. 73 (1985) 273–284. https://doi.org/10.1016/0022-3093(85)90353-9.

[6] S. Jia, H. Akamatsu, G. Hasegawa, S. Ohno, K. Hayashi, Glass-ceramic route to NASICON-type NaxTi2(PO4)3 electrodes for Na-ion batteries, Ceram. Int. 48 (2022) 24758–24764. https://doi.org/10.1016/j.ceramint.2022.05.125.

[7] M.G. Moustafa, M.M.S. Sanad, M.Y. Hassaan, NASICON-type lithium iron germanium phosphate glass-ceramic nanocomposites as anode materials for lithium ion batteries, J. Alloys Compd. 845 (2020) 156338. https://doi.org/10.1016/j.jallcom.2020.156338.

[8] Y. Shao, G. Zhong, Y. Lu, L. Liu, C. Zhao, et al., A novel NASICON-based glass-ceramic composite electrolyte with enhanced Na-ion conductivity, Energy Storage Mater. 23 (2019) 514–521. https://doi.org/10.1016/j.ensm.2019.04.009.

[9] H. Gan, W. Zhu, L. Zhang, Y. Jia, Zr doped NASICON-type LATP glass-ceramic as a super-thin coating onto deoxidized carbon wrapped CNT-S cathode for lithium-sulphur battery, Electrochim. Acta. 423 (2022) 140567. https://doi.org/10.1016/j.electacta.2022.140567.

[10] S. Saffirio, M. Falco, G.B. Appetecchi, F. Smeacetto, C. Gerbaldi, Li1.4Al0.4Ge0.4Ti1.4(PO4)3 promising NASICON-structured glass-ceramic electrolyte for all solid state Li-based batteries: Unravelling the effect of diboron trioxide, J. Eur. Ceram. Soc. 42 (2022) 1023–1032. https://doi.org/10.1016/j.jeurceramsoc.2021.11.014.

[11] C. Leo, B.V.R. Chowdari, G.V. Rao, J.L. Souquet, Lithium conducting glass-ceramics with NASICON structure, Mater. Res. Bull. 37 (2002) 1419–1430. https://doi.org/10.1016/S0025-5408(02)00793-6.

[12] R.P. Rao, C. Maohua, S. Adams, Preparation and characterization of Nasicon type Li ionic conductor, J. Solid State Electr. 16 (2012) 3349–3354. https://doi.org/10.1007/s10008-012-1780-x.

[13] P. Goharian, A. Aghaei, B. Eftekhari, S. Banijamali, Ionic conductivity and microstructural evaluatuion of Li2O-TiO2-P2O5-SiO2 glass-ceramics, Ceram. Int. 41 (2015) 1757–1763. https://doi.org/10.1016/j.ceramint.2014.09.121.

[14] S. Jadhav, M-S. Cho, R.S. Kalubrame, J-S. Lee, K-N. Jung, et al., Influence of B2O3 addition on the ionic conductivity of Li1.5Al0.5Ge1.5(PO4)3 glass-ceramics, J. Power Sources. 241 (2013) 502–508. https://doi.org/10.1016/j.jpowsour.2013.04.137.

[15] Z. Shamohammadi Ghahsareh, M. Rezvani, Crystallization behavior and structural evaluation of cordierite base glass-ceramic in the presence of CaO and B2O3 additives, Synth. Sinter. 2 (2022) 198–205. https://doi.org/10.53063/synsint.2022.24136.

[16] F.A. Santos, J.R.J. Delben, A.A.S.T. Delben, L. Andrade, S.M. Lima, Thermal stability and crystillization behavior of TiO2 dopped ZBLAN glasses, J. Non-Cryst Solids. 357 (2011) 2907–2910. https://doi.org/10.1016/j.jnoncrysol.2011.03.032.

[17] C.M. Muiva, S.T. Sathiaraj, J.M. Mwabora, Crystallization kinetics, glass forming ability and thermal stability in glassy chalcogenide alloys, J. Non-Cryst. Solids. 357 (2011) 3726–3733. https://doi.org/10.1016/j.jnoncrysol.2011.07.033.

[18] P.M. Manso, E.R. Losilla, M.M. Lara, M.A.G. Aranda, S. Bruque, et al., High lithium ionic conductivity in the Li1+xAlxGeyTi2-x-y(PO4)3 NASICON series, Chem. Mater. 15 (2003) 1879–1885. https://doi.org/10.1021/cm021717j.

[19] A. Chandra, A. Bhatt, A. Chandra, Ion conduction in superionic glassy electrolytes: An overview, J. Mater. Sci. Tech. 29 (2013) 193–208. https://doi.org/10.1016/j.jmst.2013.01.005.